Online Electronic Supplementary Information for:

Understanding spatial distributions: Negative density-dependence in prey causes predators to trade-off prey quantity with quality

Allert I. Bijleveld, Robert B. MacCurdy, Ying-Chi Chan, Emma Penning, Richard M. Gabrielson, John Cluderay, Eric L. Spaulding, Anne Dekinga, Sander Holthuijsen, Job ten Horn, Maarten Brugge, Jan A. van Gils, David W. Winkler, and Theunis Piersma

Table S1 Mixed-modelling results for density dependence in cockle flesh and shell mass. We analysed the effects of cockle density (m^{-2}) and length (mm) on an individual cockle's (A) relative ash-free dry mass of the flesh ($AFDM_{flesh}$), and (B) relative dry mass of the shell (DM_{shell}). Cockle density was log_{10}-transformed, and covariates were centred on their mean length (8.95 mm) and log_{10}-transformed density (3.14). The random effect estimates refer to standard deviations.

	Response variables	Random	Predictors	Estimates	SE	*P*
(A)	relative $AFDM_{flesh}$		intercept	-0.03	0.02	0.16
			density	-0.14	0.02	<0.01
			length	-0.00	0.00	0.52
			density × length	0.00	0.00	0.25
		sampling station		0.15		
		residual		0.16		
(B)	relative DM_{shell}		intercept	-0.01	0.02	0.75
			density	-0.06	0.03	0.04
			length	-0.00	0.00	0.97
			density × length	0.00	0.00	0.38
		sampling station		0.04		
		residual		0.04		

Table S2 Model selection results for the shape of resource selection functions. We analysed the same response variable with different types of prey related explanatory variables (resource landscapes): (A) cockle density (m^{-2}), (B) relative cockle ash-free dry mass of the flesh ($AFDM_{flesh}$), (C) predicted intake rates (IR, mg $AFDM_{flesh}$ s^{-1}), (D) average gizzard-mass-dependent predicted intake rates ($IR_{avg.gizzard}$, mg $AFDM_{flesh}$ s^{-1}), and (E) individual gizzard-mass-dependent predicted intake rate ($IR_{ind.gizzard}$, standardised). In order to analyse the shape of knot 'Resource Selection Functions' (RSF), we compared linear and quadratic models to the null model (intercept only). We avoided collinearity between the linear and quadratic terms by calculating orthogonal polynomials. To compare the different shapes of RSF, we calculated the log-likelihood of models by cross validation as follows [1]: We treated the 13 individuals as independent sampling units, and by excluding one individual at a time, fitted the resource selection model to this 'training' data. With this fitted model, we predicted the response of the excluded individual and calculated the log-likelihood in comparison to its observed response data. We repeated this procedure for all individuals and summed their log-likelihoods. The null-model with only an intercept had a log-likelihood of -1365.3. Comparing the log-likelihoods revealed that (as indicated in bold) the quadratic resource selection function was the best model for cockle density, relative $AFDM_{flesh}$, IR, as well as $IR_{avg.gizzard}$. Conversely, the linear model described the $IR_{ind.gizzard}$ resource selection function best. Note that the linear and quadratic terms were also imposed on the random effects (random slopes mixed-effect modelling).

	Resource landscapes	RSF shape	Log-Likelihood
(A)	cockle density (m^{-2})	linear	-1272.0
		quadratic	-1208.7
(B)	relative cockle $AFDM_{flesh}$	linear	-1257.2
		quadratic	-1208.0
(C)	predicted intake rate (IR, mg $AFDM_{flesh}$ s^{-1})	linear	-1178.0
		quadratic	-1123.3
(D)	average gizzard-mass-dependent intake rate ($IR_{avg.gizzard}$, mg $AFDM_{flesh}$	linear	-1175.6
		quadratic	1137.9
(E)	individual gizzard-mass-dependent intake rate ($IR_{ind.gizzard}$, standardised)	**linear**	-1171.1
		quadratic	-1184.5

Table S3 Parameter estimates of the best supported resource selection functions. (A) cockle density (m^{-2}), (B) relative cockle ash-free dry mass of the flesh ($AFDM_{flesh}$), (C) predicted intake rates (IR, mg $AFDM_{flesh}$ s^{-1}), (D) average gizzard-mass-dependent predicted intake rates ($IR_{avg.gizzard}$, mg $AFDM_{flesh}$ s^{-1}), and (E) individual gizzard-mass-dependent predicted intake rates ($IR_{ind.gizzard}$, standardised). We provide the fixed-effect estimates that represent the average response, and random-effect estimates that represent the individual variation in responses. Note that the estimates of the random effects are given in standard deviations.

	Resource landscape	Model part	Predictors	Estimates	SE
(A)	cockle density (m^{-2})	fixed	intercept	-9.4	0.05
			linear	53.3	6.04
			quadratic	-33.1	3.45
		random	intercept	0.0	
			linear	19.1	
			quadratic	7.6	
(B)	relative cockle $AFDM_{flesh}$	fixed	intercept	-9.8	0.07
			linear	-98.9	5.21
			quadratic	-59.8	11.87
		random	intercept	0.0	
			linear	5.3	
			quadratic	38.0	
(C)	predicted intake rates (IR, mg $AFDM_{flesh}$ s^{-1})	fixed	intercept	-10.2	0.17
			linear	122.8	14.56
			quadratic	-43.9	3.63
		random	intercept	0.5	
			linear	46.7	
			quadratic	2.9	
(D)	average gizzard-mass-dependent predicted intake rates ($IR_{avg.gizzard}$, mg $AFDM_{flesh}$ s^{-1})	fixed	intercept	-10.2	0.12
			linear	136.1	9.43
			quadratic	-36.4	4.26
		random	intercept	0.0	
			linear	16.7	
			quadratic	6.9	
(E)	individual gizzard-mass-dependent predicted intake rates ($IR_{ind.gizzard}$, standardised)	fixed	intercept	-9.7	0.09
			linear	91.1	7.92
		random	intercept	0.2	
			linear	23.1	

Appendix S1

Details on cockle sampling and how we measured cockle flesh and shell mass. At each sampling site we collected 0.018 m^2 of mudflat to a depth of 30 cm. Judging their length in the field, we stored cockles < 8 mm in a 4% formaldehyde solution, and froze larger cockles [2]. The cockles were often too small to separate their flesh from their shell. In those cases, we measured ash-free dry mass of whole individuals ($AFDM_{total}$). To acquire $AFDM_{flesh}$ for these individuals, we subtracted ash-free dry mass of the shell ($AFDM_{shell}$) from $AFDM_{total}$. We estimated $AFDM_{shell}$ in mg from length as $0.0047 \times mm^{2.78}$ [3]. To reduce measurement error in $AFDM_{flesh}$ of small cockles, we pooled similarly sized cockles and calculated average $AFDM_{flesh}$.

Fig. S1

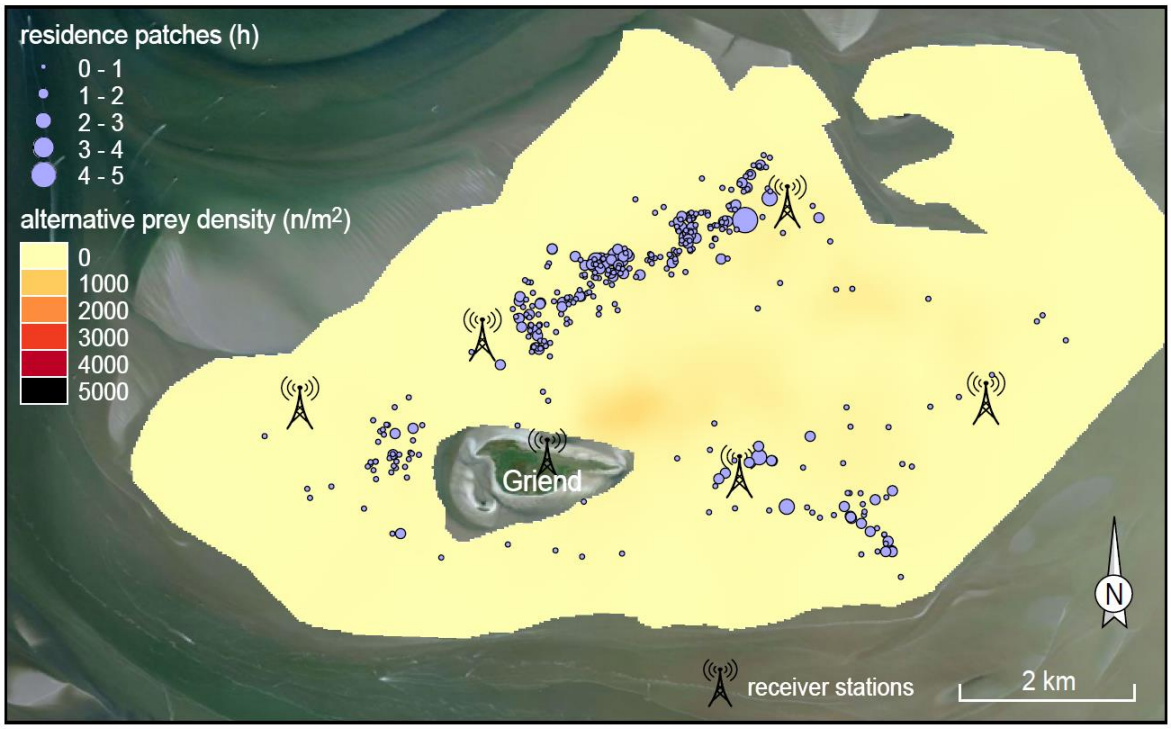

The spatial distribution of alternative prey densities. The average density of alternative prey was 33 m^{-2} (95% CI [9.6; 63.7]) and low compared to those of edible cockles (Fig. 3A). Of the prey occurring in our sampling cores, knots are known to forage on Balthic tellins (*Macoma balthica*), sand gapers (*Mya arenaria*), and *Abra tenuis*. We selected individuals of these species, which knots could swallow (length < 18 mm, [4]), summed the numbers of individuals per sampling core, and calculated densities as described in the Methods for edible cockles (*Cerastoderma edule*).

Fig. S2

Sampling methodology. (A) Photo of a tagged knot moments after its release, and (B) an overview of the study area with the array of (9) receiver stations and sampling stations. We calculated cockle densities for all sampling stations, and when cockles were found we also measured their lengths. From a subset of sampling stations, we additionally measured cockle flesh and shell mass. These stations are indicated in orange. The underlying satellite imagery was obtained from Bing in the QGIS OpenLayers plugin.

Fig. S3

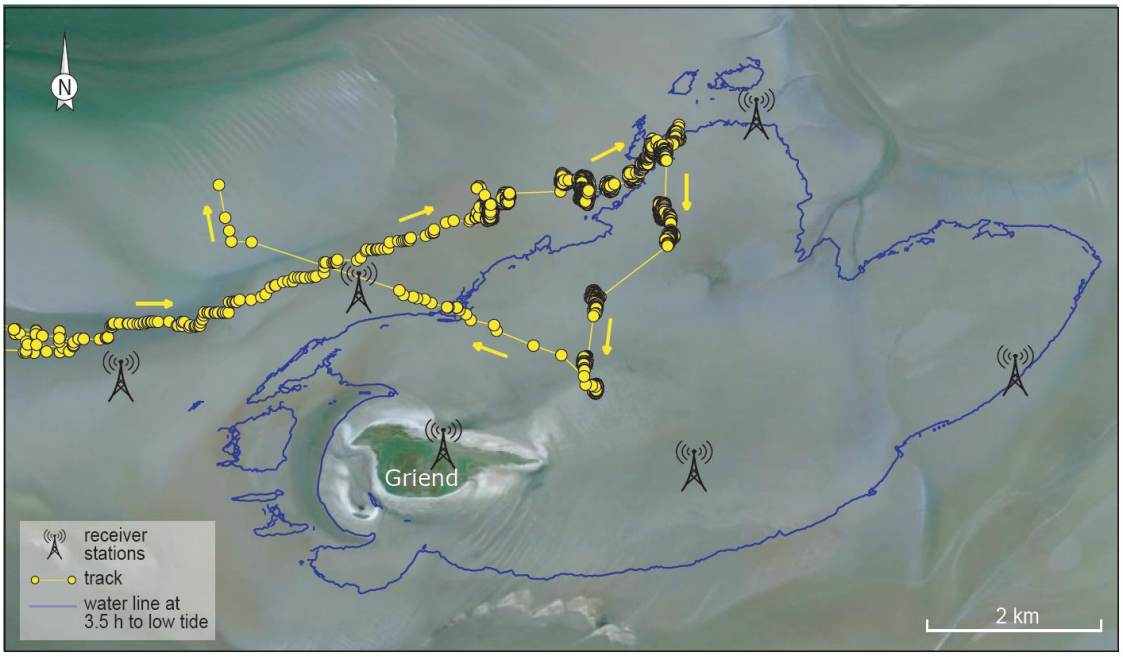

A characteristic knot movement pattern around low tide. This track was measured on 15 August 2011. The dots represent estimated positions that are connected by lines, and the arrows indicate the direction of movement. After roosting nearby on Richel (see Online Supplementary Fig. S2B) and by the time the receding water level had exposed suitable foraging grounds, the bird arrived on the mudflats north of Griend and carried on towards the northeast. With the incoming tide, it moved to the elevated mudflats northeast of Griend before flying back to Richel. The underlying satellite imagery was obtained from Bing in the QGIS OpenLayers plugin.

Fig. S4

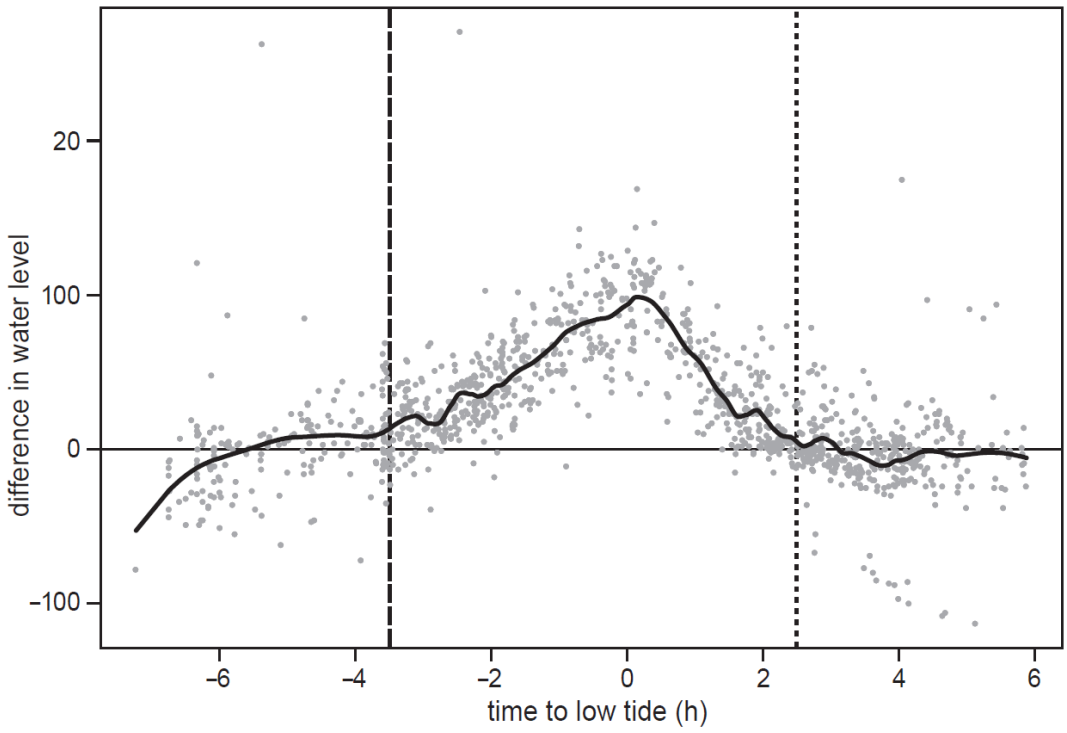

Tidal forcing on the spatial distributions of knots. Each dot represents a residence patch. The y-axis shows the difference (cm) between the water level and the height of the mudflat where the birds were located (residence patches). A positive difference indicates that birds were located on exposed mudflat. Negative values indicate that birds were standing in the water. The time to low tide (h) is shown on the x-axis. The solid line is a LOESS-fit to guide the eye. Between the long-dashed and short-dashed line there was minimal tidal forcing and the birds were more or less free to choose where to forage. The tidal data were collected by Rijkswaterstaat at West-Terschelling (53°21.45'N, 5°13.13'E) at an interval of 10 min (http://www.rijkswaterstaat.nl). The heights of the mudflats were obtained from Rijkswaterstaat as well and were collected between 2003-2008.

Fig. S5

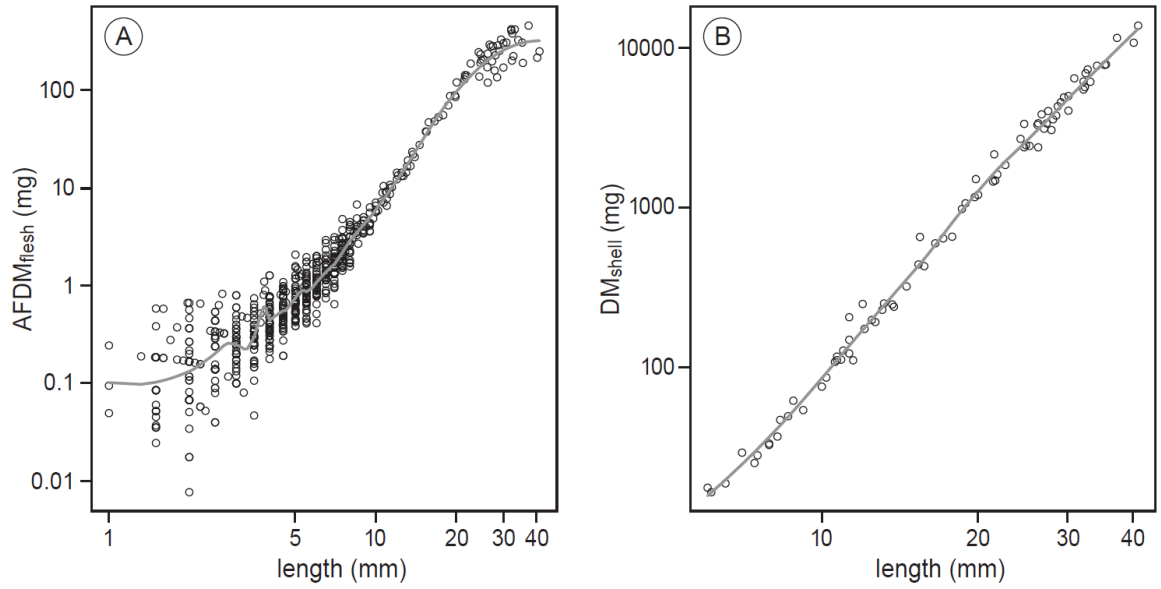

Allometric relations for cockle (A) ash-free dry mass of the flesh ($AFDM_{flesh}$), and (B) dry mass of the shell (DM_{shell}). Because of remaining non-linearity in these allometric relationships, we fitted non-linear local regression models (LOESS, solid lines) on log-log scales [5]. We used smoothing parameters of 0.2 and 0.5 for the LOESS models visualized in respectively panels A and B. We obtained an individual's relative $AFDM_{flesh}$ and DM_{shell} by back-transforming its residual from these LOESS regression models.

Fig. S6

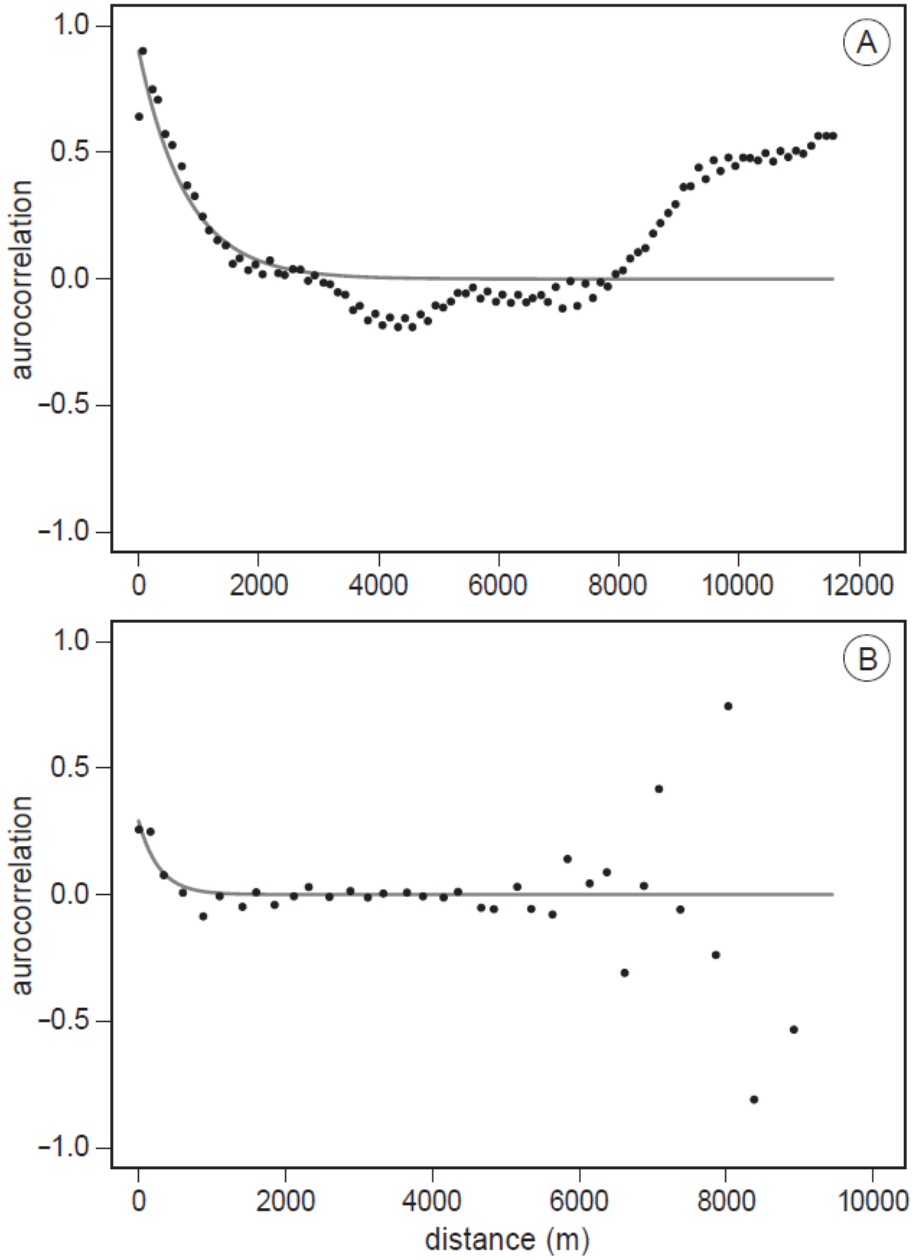

Spatial autocorrelation functions (correlograms) underlying the resource landscapes. In (A) we present the correlogram for cockle density. In (B) we present the correlogram of a cockle's relative ash-free dry mass of flesh ($AFDM_{flesh}$). The spatial autocorrelation function for density is given by $y = 0.90e^{-0.001x}$, and for relative $AFDM_{flesh}$ by $y = 0.29e^{-0.004x}$. For calculating the correlograms, we chose a spatial lag of half that of the inter-sampling distance, i.e. 125 m for interpolating densities and 250 m for interpolating relative $AFDM_{flesh}$.

Fig. S7

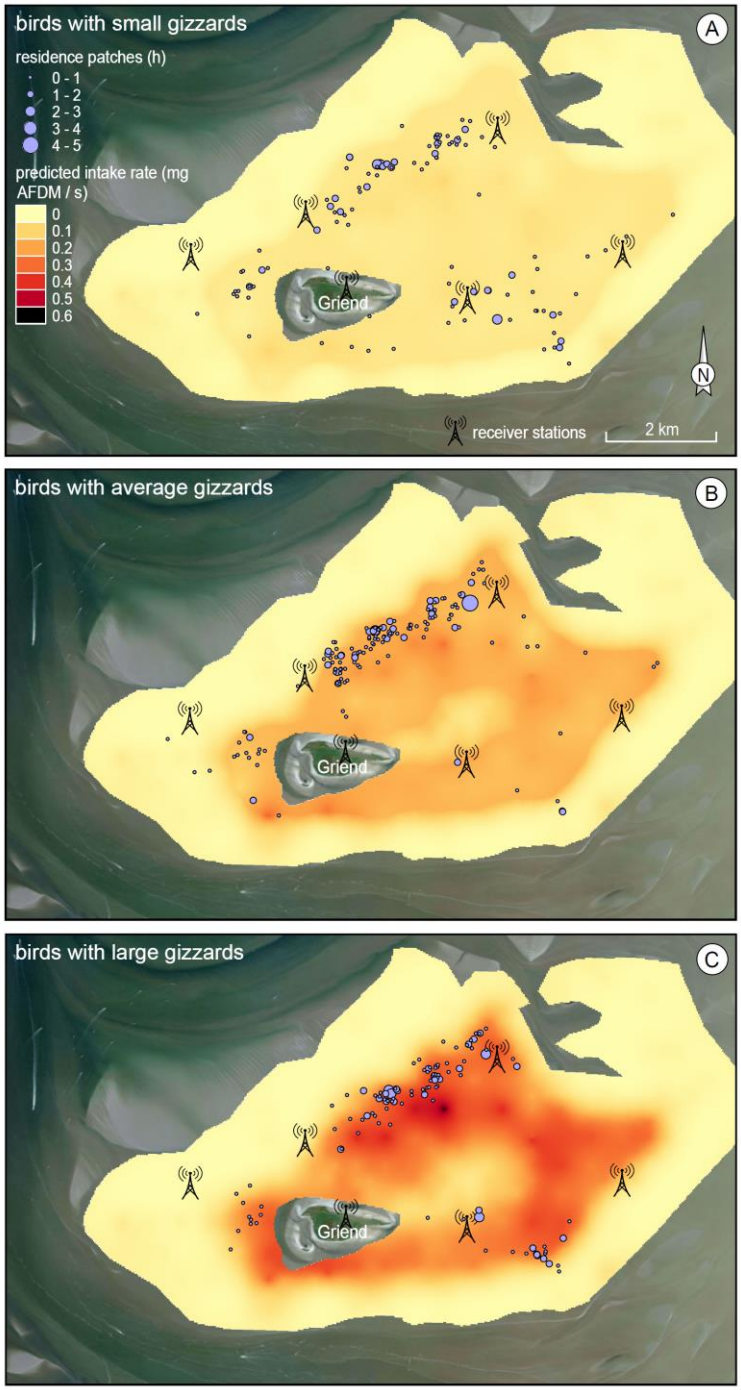

Individual gizzard-mass-dependent predicted intake rates ($IR_{ind.gizzard}$). We plotted the $IR_{ind.gizzard}$ landscapes for three hypothetical birds: (A) a bird with a small gizzard (4 gram), (B) an average gizzard (7 gram), and (C) a large gizzard (10 gram). In order to visualise the difference in predicted intake rates between birds with differently sized gizzards, we used the same colour scaling between panels. We additionally plotted the residence patches of the tagged knots with (A) gizzards < 6 g, (B) gizzards > 6 g and < 8 g, and (C) gizzards > 8 g. The sizes of these residence patch symbols indicate how long a bird had spent in that

particular location ranging from 10 min to 4.7 h. Note that the resource landscape of panel B is identical to Fig. 3D. The underlying satellite imagery was obtained from Bing in the QGIS OpenLayers plugin.

Fig. S8

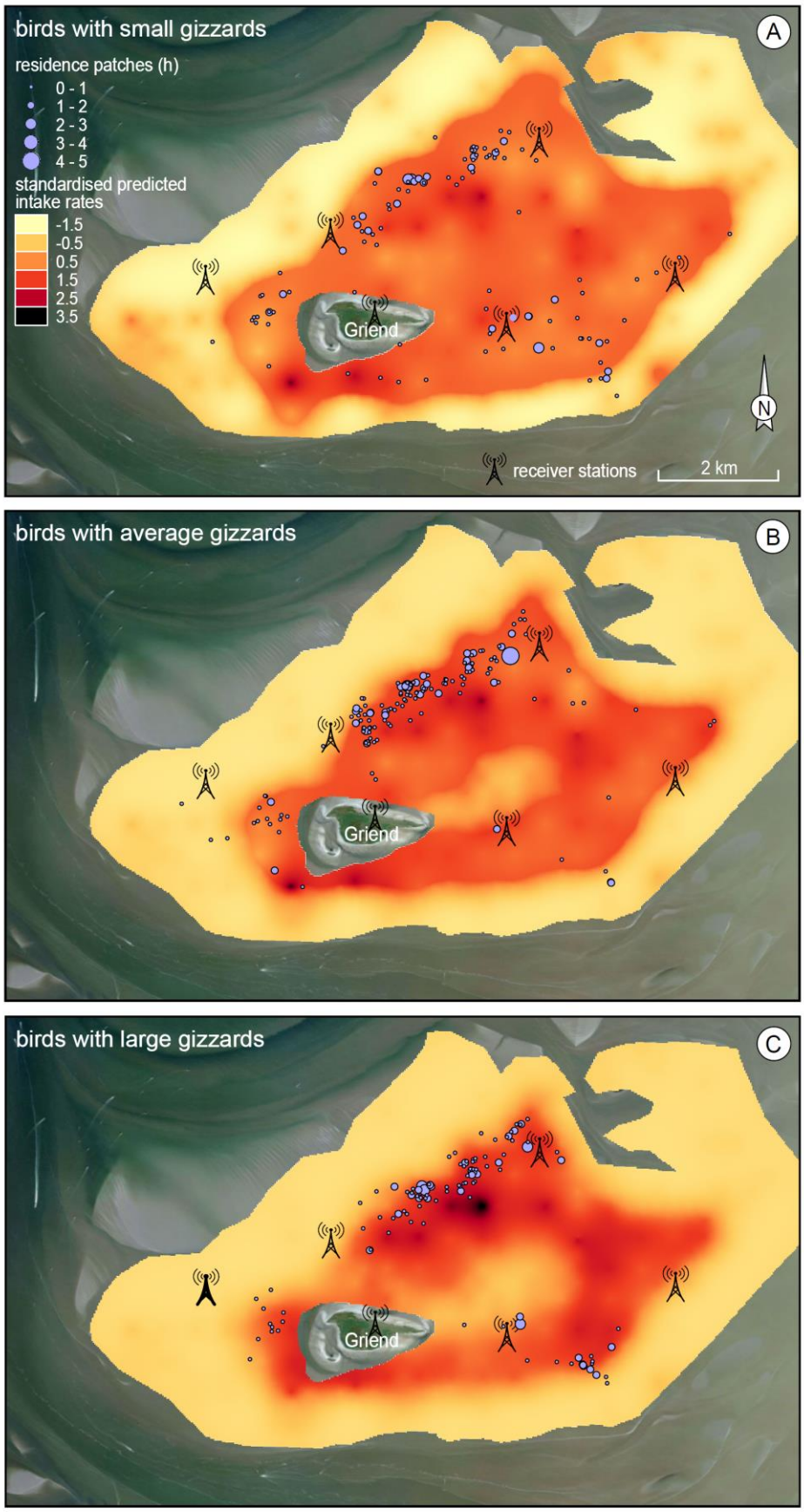
birds with small gizzards
A
residence patches (h)
0 - 1
1 - 2
2 - 3
3 - 4
4 - 5
standardised predicted intake rates
-1.5
-0.5
0.5
1.5
2.5
3.5
Griend
N
receiver stations
2 km
birds with average gizzards
B
Griend
birds with large gizzards
C
Griend

Resource landscapes of an individual‘s gizzard-mass-dependent predicted intake rates ($IR_{ind.gizzard}$, standardised). We plotted the standardised $IR_{ind.gizzard}$ landscape for three hypothetical birds: (A) a bird with a small gizzard (4 gram), (B) an average gizzard (7 gram), and (C) a large gizzard (10 gram). We superimposed the residence patches of the tagged birds with (A) gizzards < 6 g, (B) gizzards > 6 g and < 8 g, and (C) gizzards > 8 g. The sizes of these residence-patch symbols indicate how long a bird had spent in that particular location ranging from 10 min to 4.7 h. Note that the resource landscape in panel B is the standardised resource landscape of Fig. 3D. The underlying satellite imagery was obtained from Bing in the QGIS OpenLayers plugin.

Fig. S9

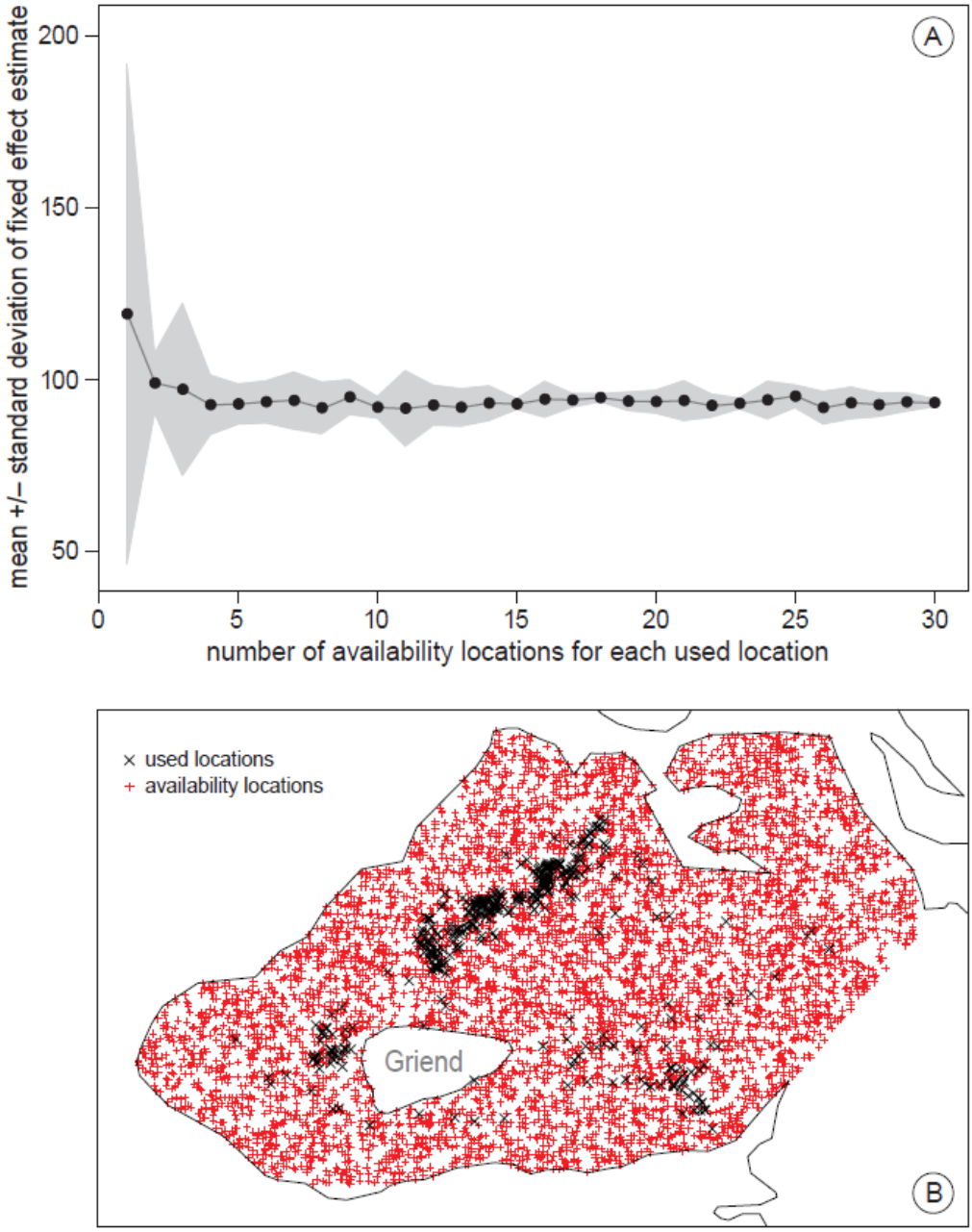

Methodology of the used-availability analyses. In order to determine the number of randomly selected availability locations, we conducted a sensitivity analysis on the fixed-effect parameter estimates. (A) An example of the sensitivity analyses on resource selection modelling. Here, we show the standard deviation (based on 5 estimates) of the linear fixed-effect estimate of the individual-gizzard-mass dependent predicted intake rate model ($IR_{ind.gizzard}$). The x-axis gives the number of availability locations for each used location. The mean of the fixed-effect and its standard deviation levelled off with the ratio of availability locations to used locations; we selected a ratio of 15 that provides reliable model estimates. (B) Map of the used and availability locations underlying our resource selection analyses.

Fig. S10

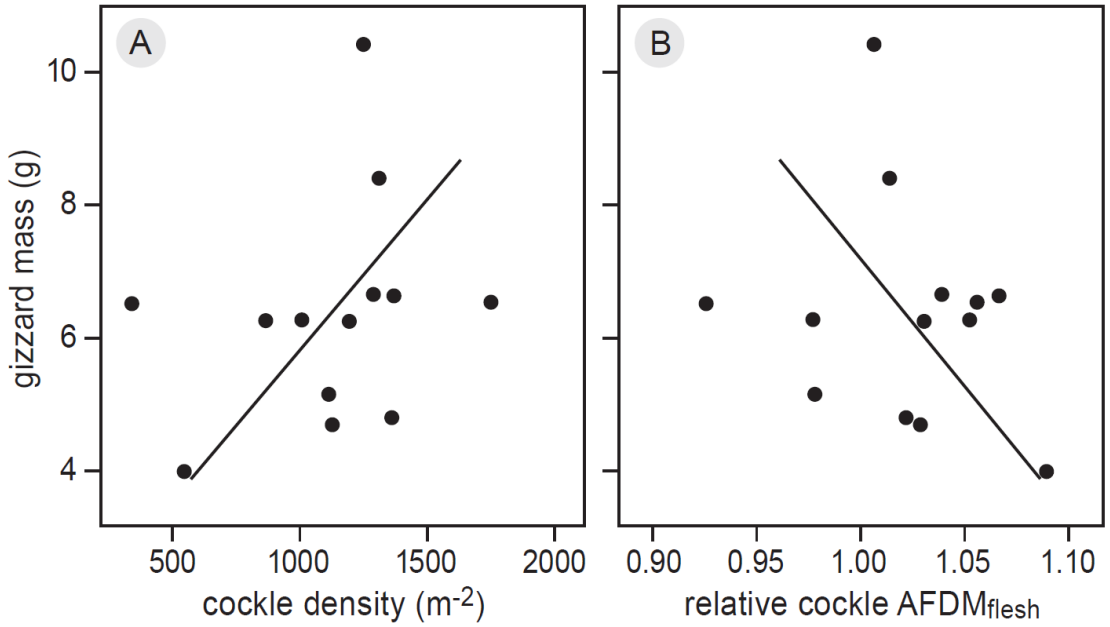

Resource selection in relation to gizzard mass. In Fig. 4E we statistically showed that knots selected those locations where they maximised their gizzard-mass-dependent energy intake rate. To intuitively illustrate that knots with different gizzard masses indeed selected locations with different cockle density and relative ash-free dry mass of the flesh ($AFDM_{flesh}$), we plot an individual's gizzard mass against its average selected (A) cockle density, and (B) relative $AFDM_{flesh}$. Indicative of a trade-off between the quantity and quality of cockle prey, we found a positive correlation between gizzard mass and cockle density, and a negative correlation between gizzard mass and relative $AFDM_{flesh}$. Each dot represents an individual. We calculated average selected cockle density and relative $AFDM_{flesh}$ by first averaging within tides and then between tides. The lines represent best-fits from standardized major axis analyses [6] calculated with the R-package "smatr".

Fig. S11

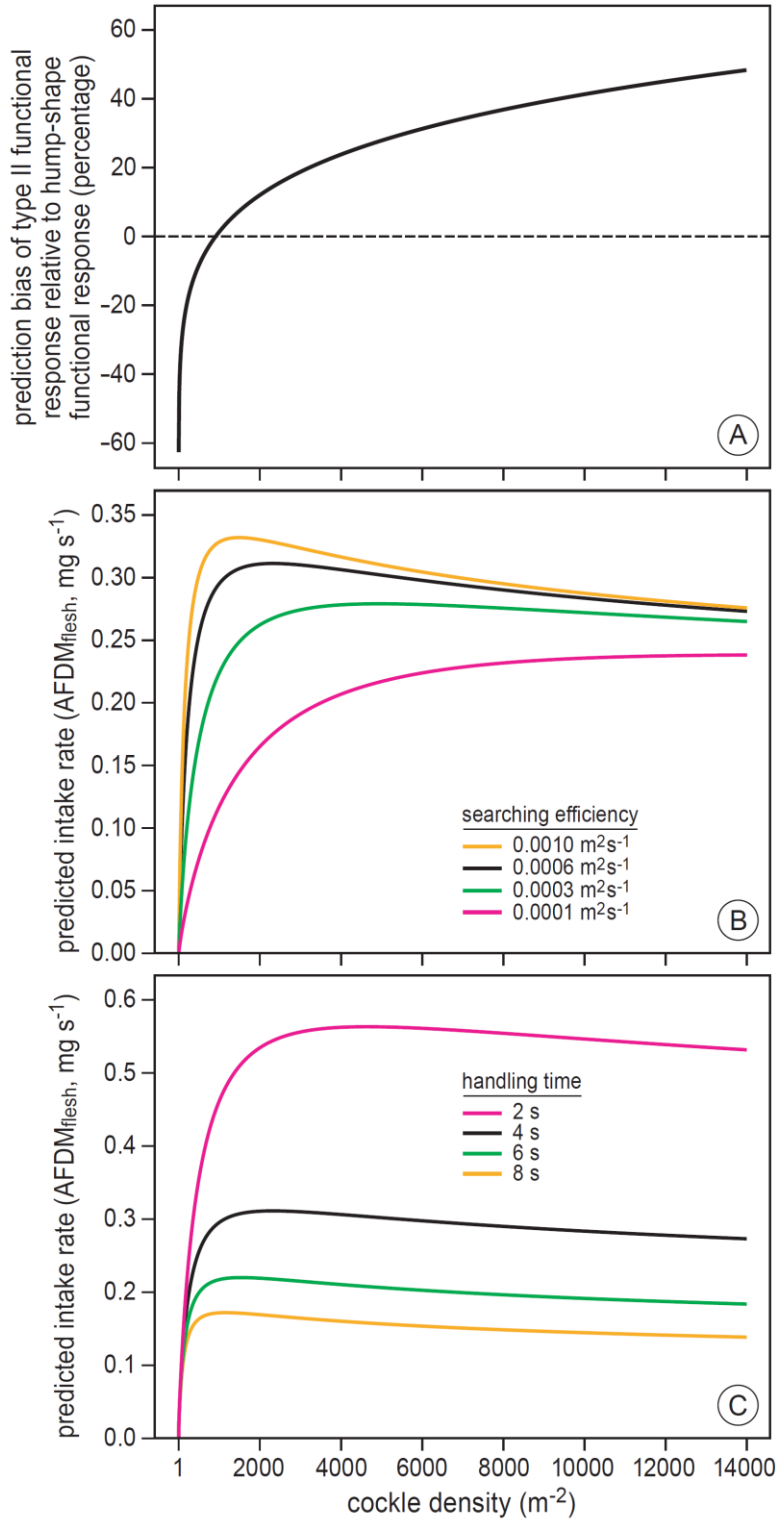

Sensitivity analyses of the type IV functional response. (A) Bias in predicted intake rates when ignoring negative density-dependence in flesh mass among prey. We calculated the difference between predicted intake rates with and without negative density dependence, and show this difference as a percentage of predicted intake rates including negative density-

dependence. This bias did not differ between model parameters (searching efficiencies and handling times) of the functional response. (B) The effect of searching efficiency on the functional response while fixing handling time at 4 s. (C) The effect of handling time on the functional response while fixing searching efficiency at 0.00064 m^2 s^{-1}. Note that we assumed equal strengths of density dependence in these sensitivity analyses, and that black lines indicate parameter values equal to those used and found in our current study.

References

1. Aarts G., Fieberg J., Brasseur S., Matthiopoulos J. 2013 Quantifying the effect of habitat availability on species distributions. *J Anim Ecol* **82**, 1135-1145. (doi:10.1111/1365-2656.12061).

2. Compton T.J., Holthuijsen S., Koolhaas A., Dekinga A., ten Horn J., Smith J., Galama Y., Brugge M., van der Wal D., van der Meer J., et al. 2013 Distinctly variable mudscapes: distribution gradients of intertidal macrofauna across the Dutch Wadden Sea. *J Sea Res* **82**, 103-116. (doi:10.1016/j.seares.2013.02.002).

3. Zwarts L. 1991 Seasonal-variation in body-weight of the bivalves *Macoma balthica, Scrobicularia plana, Mya arenaria* and *Cerastoderma edule* in the Dutch Wadden Sea. *Neth J Sea Res* **28**, 231-245.

4. Piersma T., Hoekstra R., Dekinga A., Koolhaas A., Wolf P., Battley P.F., Wiersma P. 1993 Scale and intensity of intertidal habitat use by knots *Calidris canutus* in the Western Wadden Sea in relation to food, friends and foes. *Neth J Sea Res* **31**, 331-357.

5. Bijleveld A.I., Twietmeyer S., Piechocki J., van Gils J.A., Piersma T. 2015 Natural selection by pulsed predation: survival of the thickest. *Ecology* **96**, 1943-1956. (doi:10.1890/14-1845.1).

6. Smith R.J. 2009 Use and misuse of the reduced major axis for line-fitting. *Am J Phys Anthropol* **140**, 476-486. (doi:10.1002/ajpa.21090).